

A Two-Coordinate Iron(II) Imido Complex with NHC Ligation: Synthesis, Characterization, and Its Diversified Reactivity of Nitrene Transfer and C–H Bond Activation

Jun Cheng,[†] Jian Liu,[†] Xuebing Leng,[†] Thomas Lohmiller,[‡] Alexander Schnegg,[§] Eckhard Bill,[§] Shengfa Ye,^{*,||} and Liang Deng^{*,†,||}

[†]State Key Laboratory of Organometallic Chemistry, Center for Excellence in Molecular Synthesis, Shanghai Institute of Organic Chemistry, University of Chinese Academy of Sciences, Chinese Academy of Sciences, 345 Lingling Road, Shanghai 200032, People's Republic of China

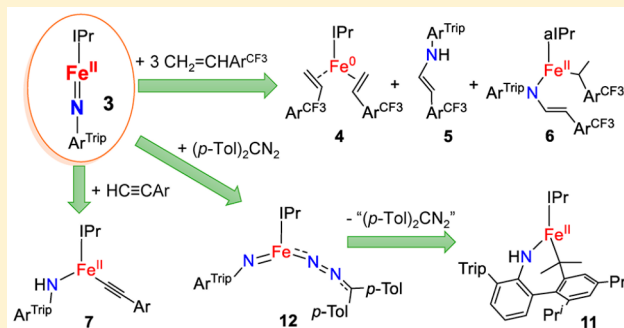
[‡]Berlin Joint EPR Lab, Helmholtz-Zentrum Berlin für Materialien und Energie, Berlin, Germany

[§]Max-Planck-Institut für Chemische Energiekonversion, Mülheim an der Ruhr D-45470, Germany

^{||}Max-Planck-Institut für Kohlenforschung, Kaiser-Wilhelm-Platz 1, Mülheim an der Ruhr D-45470, Germany

Supporting Information

ABSTRACT: Iron terminal imido species are typically implicated as reaction intermediates in iron-catalyzed transformations. While a large body of work has been devoted to mid- and high-valent iron imidos, to date the chemistry of iron(II) imidos has remained largely unexplored due to the difficulty in accessing them. Herein, we present a study on the two-coordinate iron(II) imido complex [(IPr)Fe(NAr^{Trip})] (**3**; IPr = 1,3-bis(2',6'-diisopropylphenyl)imidazol-2-ylidene; Ar^{Trip} = 2,6-bis(2',4',6'-triisopropylphenyl)phenyl) prepared from the reaction of an iron(0) complex with the bulky azide Ar^{Trip}N₃. Spectroscopic investigations in combination with DFT calculations established a high-spin *S* = 2 ground spin state for **3**, consistent with its long Fe–N multiple bond of 1.715(2) Å revealed by X-ray diffraction analysis. Complex **3** exhibits unusual activity of nitrene transfer and C–H bond activation in comparison to the reported iron imido complexes. Specifically, the reactions of **3** with CH₂=CHAr^{CF3}, an electron-deficient alkene, and CO, a strong π acid, readily afford nitrene transfer products, Ar^{CF3}CH=CHNHar^{Trip} and Ar^{Trip}NCO, respectively, yet no similar reaction occurs when **3** is treated with electron-rich alkenes and PMe₃. Moreover, **3** is inert toward the weak C(sp³)–H bonds in 1,4-cyclohexadiene, THF, and toluene, whereas it can cleave the stronger C(sp)–H bond in *p*-trifluoromethylphenylacetylene to form an iron(II) amido alkyne complex. Interestingly, intramolecular C(sp³)–H bond functionalization was observed by adding (*p*-Tol)₂CN₂ to **3**. The unique reactivity of **3** is attributed to its low-coordinate nature and the high negative charge population on the imido N atom, which render its iron–imido unit nucleophilic in nature.



INTRODUCTION

Iron terminal imido species are often implicated as key intermediates in iron-catalyzed nitrogen-group-transfer reactions: e.g., alkene aziridation, sulfur imidation, and C–H bond amination.^{1–6} A range of iron-mediated nitrogen fixation reactions have also proposed with iron imido species as intermediates en route to the final products, NH₃ and N(SiMe₃)₃.^{7–10} The importance of these chemical transformations has attracted great interest in the formation, structural and spectroscopic features, and reactivity of iron imido species. Traditional wisdom had viewed such complexes as highly reactive, nonisolable intermediates, and this knowledge had been largely restricted to theoretical and mass spectrometry studies on the bare iron imide [FeNH]⁺.¹¹ Recent studies showed that, by the use of appropriate ancillary

ligands, iron terminal imido species can be effectively stabilized and are amenable to isolation. Since Lee's report on the first isolable iron terminal imido complex, [Fe₄(μ₃-NBu^t)₄(NBu^t-Cl₃)]₃, in 2000,¹² more than 50 structurally well characterized iron terminal imido complexes have been reported.^{13–39} In addition, modern spectroscopic methods have enabled probing iron imido species that merely persist at low temperatures,^{40–42} further enriching our knowledge of this type of metal–ligand multiple-bond species.

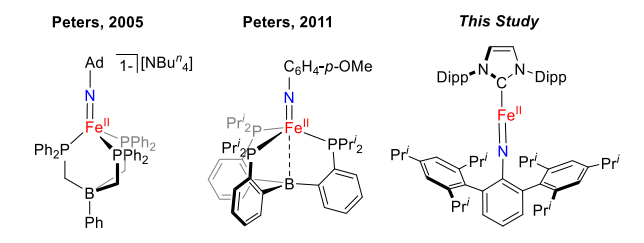
So far, the known iron imido complexes span a series of oxidation states ranging from iron(V) to iron(II).^{2,11–41} Among them, mid- to high-valent iron species, iron(V),^{20,41}

Received: April 19, 2019

Published: May 14, 2019

iron(IV),^{18,30,31,33,36,40} and iron(III) imidos^{13,17,22,35,37,38} and iminyls^{27,35} have been subjected to intensive studies, and diversified reactivity, for example nitrene transfer to CO,^{13,22} isocyanides,²² and phosphine,^{22,37} alkene aziridation,⁴³ hydrogen atom abstraction (HAA),^{16,24,28,33,42,44} and C–H bond amination,^{6,27,35,37} has been observed. In general, the nitrogen groups in high-valent iron imidos are found to be electrophilic in character.^{2,4} In contrast, few explorations on iron(II) imido species have been published. To our knowledge, Peters' complexes with trisphosphine ligation $[(\text{Bu}^n)_4\text{N}][(\text{PhB}(\text{CH}_2\text{PPh}_2)_3\text{Fe}(\text{NAd}))]$ ¹⁵ and $[(\text{B}(o\text{-C}_6\text{H}_4\text{PPr}^i_2)_3\text{Fe}(\text{NC}_6\text{H}_4\text{-}p\text{-OMe}))]$ ²⁶ (Chart 1) are the only known examples of iron(II)

Chart 1. Iron(II) Imido Complexes



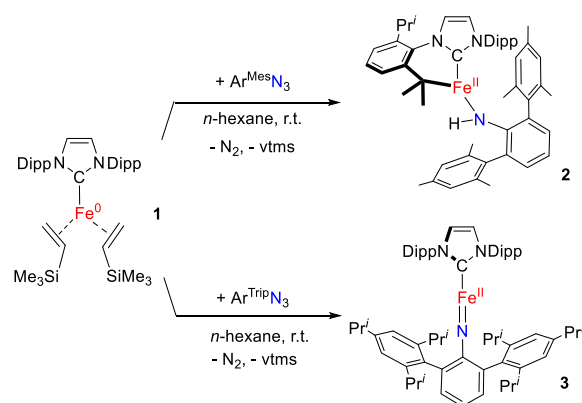
terminal imido complexes. Both iron(II) complexes exhibit a low-spin ($S = 0$) ground state. However, no reactivity study of them has been reported yet, which leaves a question as to whether iron(II) imido species are capable of performing C–H bond activation and nitrene transfer reactions that are typically found for mid- to high-valent iron imido complexes.

The aforementioned status quo prompted us to explore the chemistry of iron(II) imido species. Herein, we present a study on a two-coordinate iron(II) imido complex with N-heterocyclic carbene (NHC) ligation, $[(\text{IPr})\text{Fe}(\text{NAr}^{\text{Trip}})]$ (Chart 1), which was prepared from the reaction of its iron(0) precursor with the bulky organic azide $\text{Ar}^{\text{Trip}}\text{N}_3$. Spectroscopic characterizations and DFT calculations collectively established a high-spin ($S = 2$) ground state for iron(II) imidos. Reactivity studies revealed that the iron(II) imido complex can react with electron-deficient alkenes, e.g. 3,5-bis(trifluoromethyl)phenylethylene, to produce enamines, but it is inert toward electron-rich alkenes. Furthermore, the reactions of $[(\text{IPr})\text{Fe}(\text{NAr}^{\text{Trip}})]$ with CO and PMe_3 were found to give distinct outcomes; nitrene transfer products, an isocyanide and iron(0) species, were formed in the former reaction, whereas the ligand exchange product, the low-spin iron(II) imido complex $[(\text{Me}_3\text{P})_3\text{Fe}(\text{NAr}^{\text{Trip}})]$, was obtained for the latter. $[(\text{IPr})\text{Fe}(\text{NAr}^{\text{Trip}})]$ exhibits limited hydrogen atom abstraction activity toward 1,4-cyclohexadiene, THF, and toluene, but it is capable of activating a much stronger C(sp)–H bond to afford iron(II) amido complex when it is treated with a terminal alkyne. Interestingly, intramolecular C(sp³)–H bond activation was observed by adding an diazo compound to the iron(II) imido complex. These observations signify the unique reactivity of the iron(II) imido complex in comparison to those of mid- and high-valent iron imidos and also early-transition-metal imidos.^{2,4,45,46} The high negative charge population on the imido nitrogen atom and the low coordination number of the iron center are considered the key factors that endow the iron imido complex with such unique reactivity.

RESULTS AND DISCUSSION

Synthesis and Structure of $[(\text{IPr})\text{Fe}(\text{NAr}^{\text{Trip}})]$. Previously, we found that the reactions of the three-coordinate cobalt(0) complexes $(\text{NHC})\text{Co}(\text{vtms})_2$ (vtms = vinyltrimethylsilane) with the bulky organic azide $\text{Ar}^{\text{Mes}}\text{N}_3$ (Ar^{Mes} = 2,6-bis(2',4',6'-trimethylphenyl)phenyl) could furnish two-coordinate cobalt(II) imido complexes in the form of $(\text{NHC})\text{Co}(\text{NAr}^{\text{Mes}})$.^{47,48} Aiming to synthesize analogous iron(II) imido complexes, we examined the reaction of the three-coordinate iron(0) complex $[(\text{IPr})\text{Fe}(\text{vtms})_2]$ (**1**; IPr = 1,3-bis(2',6'-diisopropylphenyl)imidazol-2-ylidene) with $\text{Ar}^{\text{Mes}}\text{N}_3$; however, this afforded an iron(II) amide complex bearing a cyclometalated IPr ligand, $[(\text{IPr}')\text{Fe}(\text{NHAr}^{\text{Mes}})]$ (**2**) (Scheme 1). Complex **2** was isolated in high yield (75%), and its molecular structure has been confirmed by a single-crystal X-ray diffraction study (Figure S2).

Scheme 1. Reactions of $[(\text{IPr})\text{Fe}(\text{vtms})_2]$ with $\text{Ar}^{\text{Mes}}\text{N}_3$ and $\text{Ar}^{\text{Trip}}\text{N}_3$



The attainment of **2** rather than the desired iron(II) imido species $(\text{IPr})\text{Fe}(\text{NAr}^{\text{Mes}})$ hints that the iron(II) imido species might be highly reactive to initiate intramolecular C–H bond activation, which points to the necessity of further increasing steric hindrance in order to protect the FeN core. Toward this goal, the reaction of **1** with the sterically more demanding aryl azide $\text{Ar}^{\text{Trip}}\text{N}_3$ (Ar^{Trip} = 2,6-bis(2',4',6'-triisopropylphenyl)phenyl)⁴⁹ was examined, which to our delight led to the preparation of the targeted iron(II) imido complex. Specifically, treatment of **1** with 1 equiv of $\text{Ar}^{\text{Trip}}\text{N}_3$ in *n*-hexane results in the precipitation of a brown solid. After workup and recrystallization, an iron(II) imido complex, $[(\text{IPr})\text{Fe}(\text{NAr}^{\text{Trip}})]$ (**3**), was isolated in 75% yield as a brown crystalline solid (Scheme 1). Complex **3** is paramagnetic, and its measured solution magnetic susceptibility (Evans method, $\mu_{\text{eff}} = 5.5(1) \mu_{\text{B}}$ in C_6D_6 at room temperature) is close to those of the reported low-coordinate high-spin iron(II) complexes.^{50,51} The ¹H NMR spectrum of **3** (measured in C_6D_6) features 13 broad signals in the range +125 to –180 ppm (Figure S21), suggesting C_{2v} molecular symmetry. Complex **3** is air-, moisture-, and heat-sensitive. Under a dinitrogen atmosphere at room temperature, complex **3** in C_6D_6 solution showed complete decomposition in 2 days, as evidenced by the disappearance of its characteristic ¹H NMR signals. ¹H NMR analysis indicated the formation of new species, but the attempts to isolate them were unsuccessful.

A single-crystal X-ray diffraction study established the molecular structure of **3** as a two-coordinate NHC-iron-

imido complex with linear C(carbene)–Fe–N(imido)–C(aryl) alignment (Figure 1). Steric repulsion has rendered a

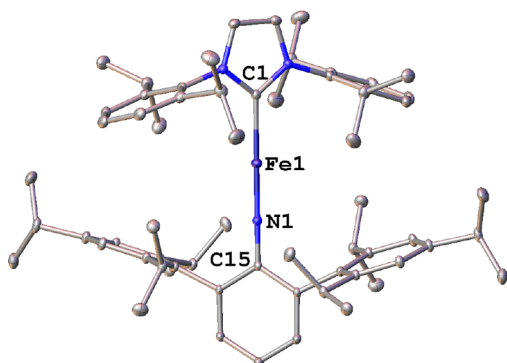


Figure 1. Molecular structure of **3**, showing 30% probability ellipsoids and the partial atom-numbering scheme. Hydrogen atoms are omitted for clarity. Selected distances (Å) and angles (deg): Fe1–N1 1.7151(16), Fe1–C1 2.0417(18), N1–C15 1.346(2); N1–Fe1–C1 180.0, C15–N1–Fe1 180.0.

staggered conformation between the core planes of the NHC ligand and the central aryl group of the imido moiety. The dihedral angle (45°) is comparable to that of the nickel complex $[(\text{IPr}^\#)\text{Ni}(\text{NAr}^{\text{Mes}})]$ (41° , $\text{IPr}^\# = 1,3\text{-bis}(2',6'\text{-bis}(\text{diphenylmethyl})\text{-4'-methylphenyl})\text{imidazol-2-ylidene}$)⁵² and apparently different from the right angle (90°) observed for $[(\text{IPr})\text{Co}(\text{NAr}^{\text{Mes}})]$.⁴⁷ Complex **3** is the first example of a two-coordinate iron(II) complex with NHC ligation.^{53,54} Its Fe–C(carbene) distance (2.042(2) Å) is found to be close to those of the two-coordinate iron(I) complexes $[(\text{cyIDep})_2\text{Fe}][\text{BAR}_4^{\text{F}}]$ (1.996(7) Å)⁵⁵ and $[(\text{IPr})\text{Fe}(\text{N}(\text{SiMe}_3)(\text{Dipp}))]$ (2.014(2) Å).⁵⁶ The Fe–N(imido) bond distance of 1.715(2) Å determined for **3** is longer than those of the low-spin iron(III), iron(IV), and iron(V) imido complexes^{2,4,20,33} and comparable to those of the high-spin iron(III) complexes $[(^{\text{Ar}}\text{DP}^{\text{Mes}})\text{Fe}^{\text{III}}(\text{NR})]$ (R = Mes, 1.708(2) Å)³⁷ and the intermediate-spin iron(III) complexes $[(\text{nacnac}^{\text{terphenyl}})\text{Fe}^{\text{III}}(\text{NAd})]$ (1.700(5) Å)²³ and $[(^{\bullet}\text{PDI}^{\text{Dipp}})\text{Fe}^{\text{III}}(\text{NAr})]$ (Ar = Dipp, 1.705(2) Å; Ar = Mes, 1.717(2) Å).¹⁷ In comparison to the low-spin iron(II) imido complexes $[\text{Bu}^n_4\text{N}][(\text{PhB}(\text{CH}_2\text{PPh}_2)_3)\text{Fe}(\text{NAd})]$ (1.651(3) Å)¹⁵ and $[(\text{B}(\text{o-C}_6\text{H}_4\text{PPr}_2)_3)\text{Fe}(\text{NC}_6\text{H}_4\text{-}p\text{-OMe})]$ (1.67 Å),²⁶ the Fe–N(imido) bond in **3** is considerably lengthened, which hints at a different electronic structure.

Spectroscopic Characterization and Electronic Structure of $[(\text{IPr})\text{Fe}(\text{NAr}^{\text{TriP}})]$. To shed light on the electronic structure of **3**, magnetometry and ^{57}Fe Mössbauer measurements coupled with DFT calculations have been undertaken.

Magnetic susceptibility measurements (Figure 2) at variable temperature with a superconducting quantum inference device (SQUID) show that the effective magnetic moment of **3** at room temperature ($\mu_{\text{eff}} \approx 6.2 \mu_{\text{B}}$) is higher than the spin-only value ($4.9 \mu_{\text{B}}$) expected for an $S = 2$ state, suggesting an unquenched orbital momentum contribution. Interestingly, with decreasing temperatures μ_{eff} first increases, and then monotonically plummets; consequently, it reaches a maximum around $6.4 \mu_{\text{B}}$ at 80 K. Similar situations were encountered for two-coordinate $S = 2$ iron(II) alkyl, amido, and aryloxo complexes.^{57–59} Our exploring simulations revealed that the overshooting behavior of μ_{eff} found for **3** originates mainly from large g -anisotropy. The variable-temperature and variable-

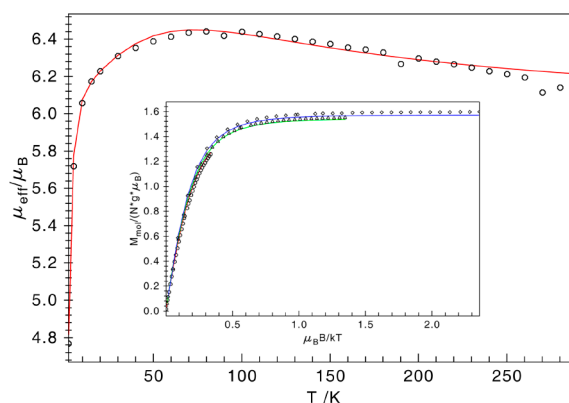


Figure 2. Temperature dependence of the effective magnetic moment, μ_{eff} , of a solid sample of **3** recorded in a 1.0 T magnetic field and variable-field and variable-temperature dependence of the magnetization of **3** (inset). The solid lines represent a reasonable fit using the following parameters: $D = -42 \text{ cm}^{-1}$, $E/D = 0.07$, $g_{\parallel} = 2.08$, and $g_{\perp} = 3.05$.

field magnetization studies revealed that all isofield curves are nearly superimposable, which reflects an exceedingly large magnetic anisotropy in **3**. The simulation of the combined SQUID data yielded $g_{\parallel} = 2.08(6)$, and $g_{\perp} = 3.05(6)$, but the D and E/D values only can be narrowed down to $D < -10 \text{ cm}^{-1}$ and $0 < E/D < 0.11$, because the computed relevant error surface is rather flat (Figures S45 and S46).

Zero-field ^{57}Fe Mössbauer measurements at various temperatures ranging from 80 to 293 K exhibited a broad and asymmetric quadrupole doublet (Figure S17), probably due to intermediate spin relaxation.⁶⁰ As depicted in Figure 3,

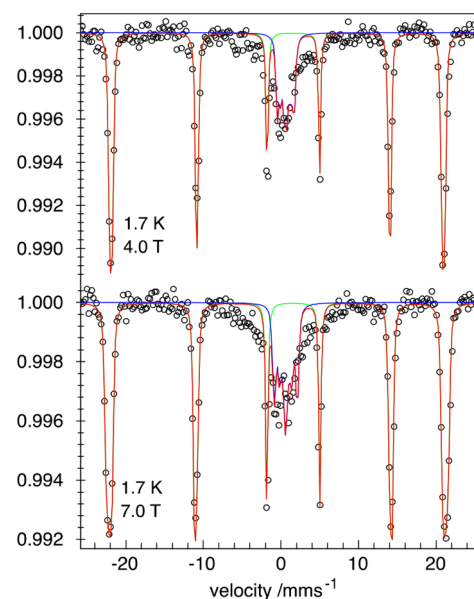


Figure 3. Variable-field magnetic Mössbauer spectra of **3** in solid state. The solid sample of **3** was immobilized in eicosane ($\text{C}_{20}\text{H}_{42}$). Fields were applied perpendicular to the γ -rays. Solid lines represent the best fit using the following parameters: $\delta = 0.56 \text{ mm/s}$, $\Delta E_{\text{Q}} = -2.08 \text{ mm/s}$, $\eta = 0$ (fixed), $A_{\parallel} = +65.8 \text{ T}$, $D = -42 \text{ cm}^{-1}$ (fixed), $E/D = 0.07$ (fixed), $g_{\parallel} = 2.08$ (fixed), and $g_{\perp} = 3.05$ (fixed). The spectra show the sample contains 25% diamagnetic impurity. However, the much sharper features of **3** can be readily identified and the existence of the impurity does not affect our further analysis.

magnetic Mössbauer spectra of complex **3** in the solid state, recorded at 1.7 K with 4.0 and 7.0 T applied perpendicular to the γ -rays, display well-resolved magnetic splitting. The relative intensity of the six lines indicates that complex **3** features extremely strong easy-axis magnetization at low temperatures. Assuming that the principal axis system of the electric field gradient tensor is largely collinear with that of D , a satisfactory fit gave $\delta = 0.56(2)$ mm/s, $\Delta E_Q = -2.08(6)$ mm/s, and $A_{\parallel} = +65.8(6)$ T. Precise determination of the D and E/D values by the applied Mössbauer measurements is hampered by fast relaxation of **3**, due to the existence of the unquenched orbital angular momentum. Therefore, during the simulations, D , E/D , g_{\parallel} and g_{\perp} were fixed to those determined by the above magnetometry investigations. The simulations do not allow accurate determination of the A_{\perp} and η values either, because nearly all ^{57}Fe nuclear spins are polarized along the z axis of the ZFS tensor. According to the observed A_{\parallel} value, complex **3** possesses an internal magnetic field of ~ 132 T. The measured Mössbauer parameters are comparable to those found for analogous two-coordinate high-spin ferrous complexes.^{61–64}

Figure 4 illustrates the electronic structure computed by B3LYP calculations. The computations predicted an electron

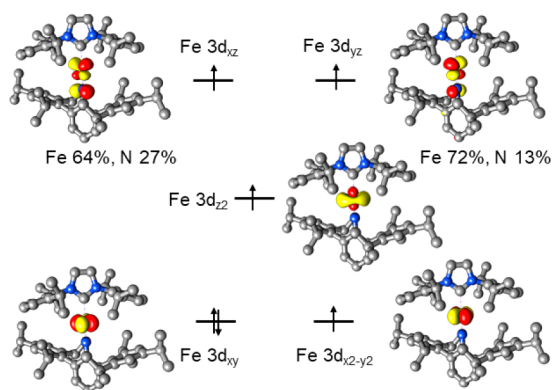


Figure 4. Frontier molecular orbital diagram of $[(\text{IPr})\text{Fe}(\text{NAr}^{\text{Trip}})]$ (**3**) derived from a B3LYP calculation.

configuration of $(d_{x^2-y^2})^2(d_{xy})^1(d_z)^1(d_{xz/yz})^2$ for the ground state of **3**. The linear coordination environment of the iron center in **3** leads to formation of two π bonds between Fe $3d_{xz/yz}$ and N $2p_{x/y}$ atomic orbitals and one σ bond between Fe $3d_z^2$ and N p_z . As borne out by the shape of the orbital labeled as Fe $3d_z^2$, significant $3d_z^2-4s$ mixing considerably reduces the antibonding interaction with the two ligand and hence stabilizes the σ^* orbital relative to the two π^* orbitals, a bonding feature found for the low-spin complex $[(\text{PhB}(\text{o}-\text{C}_6\text{H}_4\text{PPr}^i)_2)_3\text{Fe}(\text{NAd})]^+$ as well.⁴ Furthermore, the remaining Fe $3d_{x^2-y^2}$ and $3d_{xy}$ orbitals are essentially nonbonding in nature. The orbital occupation pattern of the ground state therefore defines a formal bond order of 1.5 for the Fe–N(imido) interaction. In line with this reasoning, **3** features a longer Fe–N bond distance relative to those measured for the low-spin Fe(II)-imido complexes.^{15,26} The Fe–N π interaction in **3** is somewhat ionic, as suggested by the uneven contribution of the Fe and N atomic orbitals to the two Fe–N π^* orbitals. As a consequence, the imido ligand of **3** donates less electron density to the Fe center and its N atom thus accumulates sizable negative charge. This notion is consistent with the computed charge population of N (-0.57), which is much higher than that of Fe (-0.18). Our further theoretical

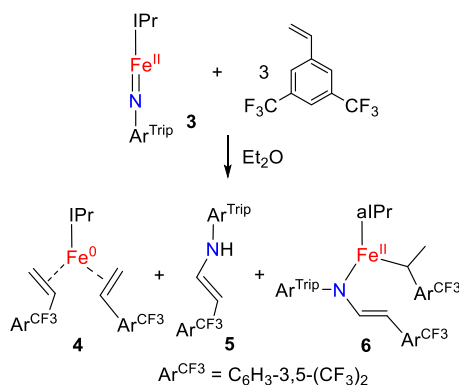
results showed that the computed negative charge population on the N atom of **3** is much higher than those of the related iron(III) imido/imino complexes $[(\text{nacnac}^{\text{terphenyl}})\text{Fe}(\text{NAd})]^{23}$ (-0.45), $[(^{\text{Ar}}\text{DP}^{\text{Mes}})\text{Fe}(\text{NMes})]^{37}$ (-0.48), and $[(^{\text{Ar}}\text{DP}^{\text{Mes}})\text{Fe}(\text{NC}_6\text{H}_4\text{-}p\text{-Bu}^t)\text{Cl}]^{27}$ (-0.38) (Table S3), which hints at stronger basicity/nucleophilicity of the imido moiety in **3**. On the basis of the metal–ligand interaction discussed above for **3**, one can envision it has a rather low lying excited state with an electron configuration of $(d_{x^2-y^2})^1(d_{xy})^2(d_z)^1(d_{xz/yz})$. A CASSCF(12,13) calculation reveals that this excited state is only 190 cm^{-1} above the ground state. Both states are hence nearly degenerate, which explains the unusual magnetic properties observed for **3**.^{61–64}

Reactivity of $[(\text{IPr})\text{Fe}(\text{NAr}^{\text{Trip}})]$. Complex **3** represents the first example of isolable iron(II) imido species featuring a high-spin ($S = 2$) ground state. As mentioned earlier, structurally well characterized iron(II) terminal imido complexes are scarce, and their chemistry has remained largely unexplored.^{15,26} The status quo thus prompted us to further investigate the reactivity of **3**.

Reactions with Alkenes. In iron-catalyzed alkene aziridation reactions, iron terminal imido complexes were proposed as key intermediates.^{44,65–68} However, isolable iron imido species capable of reacting with alkenes are exceedingly rare. The only known example is Betley's iron(III) imino complex $[(^{\text{Ar}}\text{DP}^{\text{Mes}})\text{Fe}^{\text{III}}(\bullet^-\text{NAd})\text{Cl}]$, which can react with alkenes to afford aziridines and allyl amines.⁴³ As elaborated below, complex **3** is reactive toward electron-deficient alkenes to give distinct net nitrene transfer products, enamines; more importantly, the transformation displays a disparate reactivity pattern in comparison to that observed for the iron(III) imino complexes.

Examining the reactions of **3** with different alkenes revealed the higher activity of **3** toward electron-deficient terminal alkenes over electron-rich alkenes. For instance, treatment of **3** with 3 equiv of 3,5-bis(trifluoromethyl)phenylethylene ($\text{Ar}^{\text{CF}_3}\text{CH}=\text{CH}_2$) at room temperature in Et_2O can lead to the full consumption of **3** in hours. In contrast, **3** is inert toward 4-methoxyphenylethylene, 1-octene, and 4-methylcyclohexene. Our further workup and characterization study revealed that the reaction of **3** with 3,5-bis(trifluoromethyl)phenylethylene gives a mixture of the iron(0) complex $[(\text{IPr})\text{Fe}(\text{CH}_2\text{CHAr}^{\text{CF}_3})_2]$ (**4**), the enamine $\text{trans-Ar}^{\text{CF}_3}\text{CH}=\text{CHNAr}^{\text{Trip}}$ (**5**), and the iron(II) enamino complex $[(\text{aIPr})\text{Fe}(\text{NAr}^{\text{Trip}}\text{CHCHAr}^{\text{CF}_3})(\text{CHMeAr}^{\text{CF}_3})]$ (**6**; aIPr = 1,3-bis-(2',6'-diisopropylphenyl)imidazol-4-ylidene) (Scheme 2), along with unidentified fluoro-containing species. Complex **4** has been characterized by NMR and elemental analysis. Its ^1H NMR spectrum displays a resonance pattern similar to that of **1**. The yield of **4** in this reaction is low (ca. 6% based on ^{19}F NMR analysis). On the other hand, the ligand replacement reaction of **1** with 2 equiv of $\text{Ar}^{\text{CF}_3}\text{CH}=\text{CH}_2$ proved a more reliable synthetic route for **4**. The enamine **5** was isolated in 62% yield when chromatographic separation was performed on the quenched reaction mixture. The high isolated yield of **5** partially comes from protonation of the enamino complex **6**. Compound **5** has been characterized by NMR and mass spectroscopy. Its ^1H NMR spectrum exhibits a diagnostic vicinal, trans coupling constant of 13.8 Hz for its olefinic hydrogens, and DEPT ^{13}C NMR spectra also support its identity. ^{19}F NMR analysis suggested a moderate yield (ca. 50%) for **6**. Because of its high solubility in common organic solvent, only a small amount of red crystals of **6** could be

Scheme 2. Reaction of 3 with 3,5-bis(trifluoromethyl)phenylethylene



isolated. Single-crystal X-ray diffraction established its structure as an iron(II) enamino complex (Figure 5). The enamino

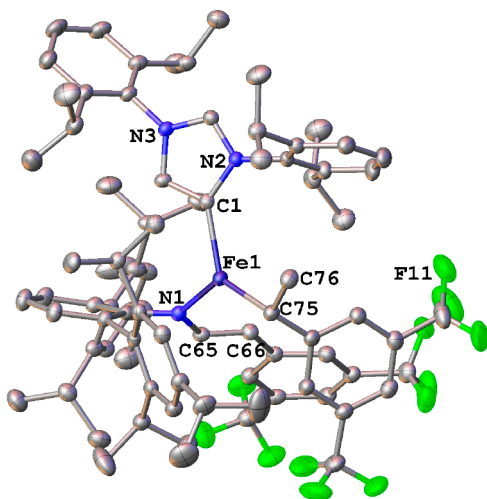


Figure 5. Molecular structure of $[(\text{aIPr})\text{Fe}(\text{NAr}^{\text{Trip}}\text{CHCHAr}^{\text{CF}_3})\text{-(CHMeAr}^{\text{CF}_3})]$ (**6**), showing 30% probability ellipsoids and the partial atom-numbering scheme. Hydrogen atoms are omitted for clarity. Selected distances (Å): Fe1–N1 2.020(3), Fe1–C1 2.111(3), Fe1–C75 2.104(3), N1–C65 1.367(4), C65–C66 1.344(5), C75–C76 1.532(5).

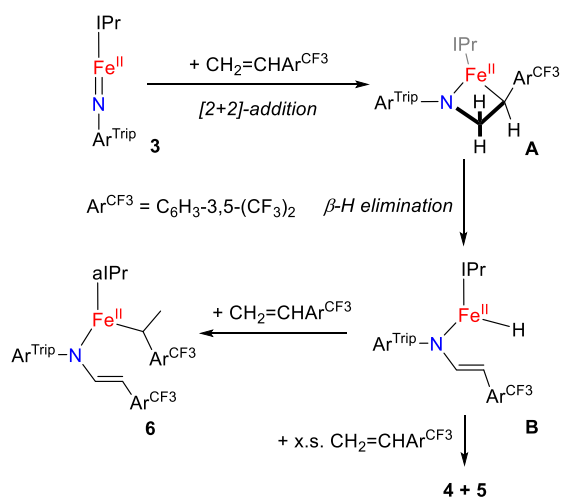
ligand in **6** has Fe–N and C65–C66 distances of 2.020(3) and 1.344(5) Å, respectively, which are typical of Fe–N single bonds and C=C double bonds. The Fe–C(75) and C(75)–C(76) distances of 2.104(3) and 1.532(5) Å, respectively, support the identity of a 1-phenyl-1-ethyl ligand. Probably driven by the relief of steric congestion, the reaction also induced the conversion of IPr into its abnormal form aIPr. Similar normal to abnormal rearrangement has been observed in three-coordinate iron(II) amido NHC complexes.⁶⁹ In addition to **4–6**, ¹⁹F NMR analysis indicated that a species which shows ¹⁹F NMR signals at –62.18 and –62.54 ppm were also formed in the reaction of **3** with $\text{Ar}^{\text{CF}_3}\text{CH}=\text{CH}_2$. However, attempts to isolate the species were unsuccessful. In addition to the reaction with 3,5-bis(trifluoromethyl)phenylethylene, complex **3** could also react with ethylene, styrene, and vinyltrimethylsilane, which are more electron rich than 3,5-bis(trimethyl)phenylethylene. The latter reactions, however, proceeded more sluggishly. GC-MS analyses on these reaction mixtures indicated the formation of new organic

species having molecular masses anticipated for the corresponding enamines. However, even when the alkenes were used in a large excess (more than 100 equiv), the yields of the desired enamines in 24 h were low (<10%), and further isolation attempts were unsuccessful.

The production of enamine in the reaction of **3** with 3,5-bis(trifluoromethyl)phenylethylene is different from the formation of aziridines in the reactions of Betley's iron(III) iminyl complexes $[(\text{Ar}^{\text{DP}^{\text{Mes}}})\text{Fe}^{\text{III}}(\text{NAd})\text{Cl}]$ with substituted styrenes.⁴³ For the latter, irrespective of electron-donating and -withdrawing groups on the para position of styrenes, all reactions showed rates accelerated over that with unsubstituted styrene. According to this finding, the aziridation reaction was proposed to proceed via the sequential steps of the attack of iminyl radical on styrenes followed by radical rebound. The different reaction outcome reflects the influence of the electronic structure of the nitrogen group, $[\text{NAr}^{\text{Trip}}]^{2-}$ in **3** versus $[\text{NAd}]^{\bullet-}$ in $[(\text{Ar}^{\text{DP}^{\text{Mes}}})\text{Fe}^{\text{III}}(\text{NAd})\text{Cl}]$, on its reactivity toward alkene. On the other hand, the distinct coordination numbers, two-coordinate in **3** over four-coordinate in $[(\text{Ar}^{\text{DP}^{\text{Mes}}})\text{Fe}^{\text{III}}(\text{NAd})\text{Cl}]$, should also be among the contributing factors, as they might induce the reaction to operate in an “inner-sphere” or “outer-sphere” pathway.^{70,71}

Although the reaction of **3** with 3,5-bis(trifluoromethyl)phenylethylene bears resemblance to the production of imine and enamine, respectively, in the reactions of $[(\text{IPr})\text{Co}(\text{NAr}^{\text{Mes}})]^{47}$ and $[(\text{IPr}^{\#})\text{Ni}(\text{NAr}^{\text{Mes}})]^{52}$ with ethylene, these divalent late 3d metal imido species seems to show differentiated affinity toward ethylene. Only low conversion was detected in the reaction of the iron(II) imido complex **3** with ethylene, whereas the reactions of cobalt(II) and nickel(II) imido complexes with ethylene took place quickly and gave the products in high conversions. This difference is likely associated with the different character of the nucleophilicity/electrophilicity of these divalent late 3d metal imido species. Our DFT calculation studies on $[(\text{IPr})\text{Fe}(\text{NAr}^{\text{Trip}})]$ (**3**), $[(\text{IPr})\text{Co}(\text{NAr}^{\text{Mes}})]$, and $[(\text{IPr}^{\#})\text{Ni}(\text{NAr}^{\text{Mes}})]$ revealed a stepwise decrease in the negative charge population on their imido N atom (–0.57, –0.51, and –0.46, respectively; see Table S3), as a consequence of the gradually increased effective nuclear charge of the metal center. Therefore, we hypothesized that the $[\text{NAr}]$ group in the iron(II) imido species is more nucleophilic or less electrophilic than those in its cobalt(II) and nickel(II) imido congeners.

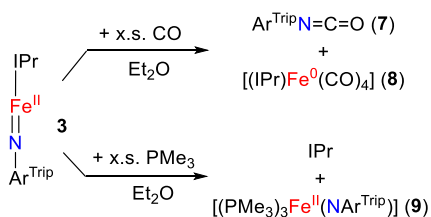
On the basis of the above discussion, we proposed the route shown in Scheme 3 to explain the production of enamine. The iron(II) imido complex **3** interacts with the alkene to give a $[2\pi + 2\pi]$ -addition product, the four-membered metallacycle **A** (Scheme 3), as usually found for early-transition-metal imido complexes.⁷² The intermediate **A** then undergoes β -H elimination to form the iron(II) enamino hydride species **B**, which eventually initiates reductive elimination to form **4** and **5** (Scheme 3).⁵² As such, **6** is generated by inserting a 3,5-bis(trifluoromethyl)phenylethylene into the Fe–H bond of enamino iron(II) intermediate **B**, accompanied by the normal to abnormal NHC rearrangement (Scheme 3). Intriguingly, the C=C double bond of the enamino ligand in **6** exhibits a trans configuration like that of **5**. This observation hints that the steric repulsion between the 3,5-bis(trifluoromethyl)phenyl group and IPr in the four-membered metallacycle **A** might govern the selectivity of the β -H elimination step. As the nitrogen atoms of amido ligands in low-coordinate iron(II) complexes usually show trigonal-planar geometry,^{33,53,73} steric

Scheme 3. Proposed Route for the Reaction of 3 with 3,5-Bis(trifluoromethyl)phenylethylene


repulsion between Ar^{Tri}p and IPr in intermediate **A** could be alleviated.

Reactions with CO and PMe₃. Nitrene transfer to CO and phosphine to form isocyanates and iminophosphines has been observed for both iron(III) and iron(IV) imido species.^{2,4,22,37} To check whether or not iron(II) imidos can perform nitrene transfer reactions with these substrates, the reactions of **3** with CO and PMe₃ were examined. It turned out that a facile transformation was observed when **3** was treated with CO, but the reaction of **3** with PMe₃ does not yield Me₃PNAr^{Tri}p.

The interaction of **3** with an excess amount of CO (1 atm) proceeded quickly and gave the nitrene transfer reaction products, the isocyanate Ar^{Tri}pNCO (**7**) and iron(0) species [(IPr)Fe(CO)₄] (**8**), in high yields (Scheme 4). The reaction

Scheme 4. Reactions of 3 with CO and PMe₃


of **3** with PMe₃, however, did not produce a nitrene transfer product but afforded ligand-replacement products, IPr and the low-spin iron(II) imido complex [(PMe₃)₃Fe(NAr^{Tri}p)] (**9**). Complex **9** displays a distorted-tetrahedral coordination geometry that is similar to those of [(PMe₃)₃Ru(NDipp)]⁷⁴ and [(PMe₃)₃Co(NAr^{Mes})]⁷⁵ (Figure 6). Its short Fe–N distance (1.675(2) Å) and nearly linear Fe–N–C alignment (171.8(3)°) resemble those of [(B(*o*-C₆H₄PPri₂))₂Fe(NC₆H₄-*p*-OMe)].²⁶ To our surprise, **9** resists further reductive elimination to form Me₃PNAr^{Tri}p even when a mixture of **9** with 20 equiv of PMe₃ in benzene is heated at 60 °C for 36 h.

Nitrene-transfer reactions of metal–ligand multiple bond species with phosphines involves orbital interactions of the frontier molecular orbitals of metal–ligand multiple-bond species with the lone pair and σ*(C–P) orbital of phosphines. This notion is well-demonstrated in the nitrogen atom transfer reaction of iron(V) nitrido with PPh₃ by Smith and Harvey.⁷⁶ Alkyl phosphines as σ-donating ligands possess rather limited

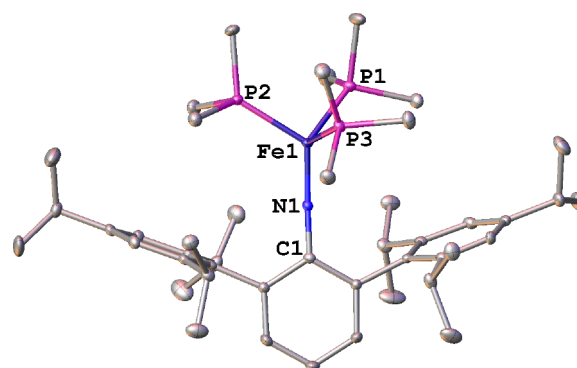
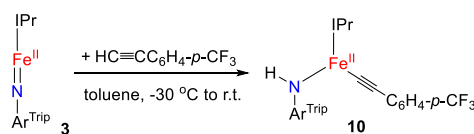


Figure 6. Molecular structure of [Fe(NAr^{Tri}p)(PMe₃)₃] (**9**), showing 30% probability ellipsoids and the partial atom-numbering scheme. Hydrogen atoms are omitted for clarity. Selected distances (Å) and angles (deg): Fe1–P1 2.1726(10), Fe1–P2 2.1685(9), Fe1–P3 2.1342(10), Fe1–N1 1.675(2), N1–C1 1.380(3); N1–Fe1–P1 125.97(10), N1–Fe1–P2 122.33(9), N1–Fe1–P3 110.85(11), P2–Fe1–P1 96.64(4), P3–Fe1–P1 96.57(4), P3–Fe1–P2 98.77(4), C1–N1–Fe1 171.8(3).

π-accepting ability (high lying σ*(C–P) orbital), whereas CO has pronounced σ-donating and also good π-accepting ability. On the basis of this consideration, again we attributed the reaction product not being Me₃PNAr^{Tri}p to the essentially nucleophilic nature of the imido moiety in **3**, in striking contrast to mid- and high-valent iron imido/imidyl species. Interestingly, the low-spin iron(II) imido complex **9** was also found to be inert toward 3,5-bis(trifluoromethyl)phenylethylene. This finding is consistent with the notion that the nucleophilicity of the imido moiety in **3** plays an important role in functionalizing C=C bonds, because the calculated negative charge population on the imido nitrogen of **9** (−0.46) is lower than that of its counterpart in **3** (−0.57) (Table S3).

C–H Bond Activation Reactions. Facile hydrogen atom abstraction (HAA) reactions^{77,78} have been observed for iron(V),⁴² iron(IV),^{33,39,40,79–81} and iron(III) imido^{37,50,82} species. In this regard, we have also tested the activity of **3** toward cleaving C–H bonds in a range of hydrocarbons with different C–H bond strengths and found that **3** is able to activate a C(sp)³–H bond but is inert toward the substrates with weaker C(sp³)–H bonds.

The reaction of **3** with a terminal alkyne, *p*-trifluoromethylphenylacetylene, forms the iron(II) amido alkynyl complex [(IPr)Fe(NHAr^{Tri}p)(CCC₆H₄-*p*-CF₃)] (**10**; Scheme 5). The

Scheme 5. Reaction of 3 with *p*-CF₃C₆H₄CCH


structure of **10** was established by a single-crystal X-ray diffraction study (Figure 7). The presence of a terminal alkynyl ligand, a long Fe–N(amido) distance of 1.922(2) Å, and a bent Fe–N(amido)–C(aryl) angle of 139.24(19)° in **10** clearly indicated the occurrence of C(sp)³–H bond activation in this reaction. On the other hand, no reaction occurred when **3** was treated with THF, toluene, or 1,4-cyclohexadiene (CHD) at room temperature despite the presence of weaker

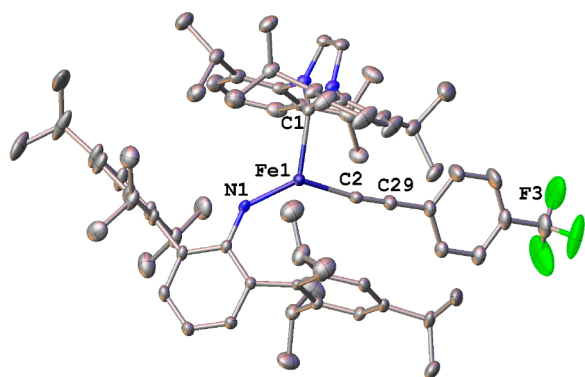


Figure 7. Molecular structure of $[(\text{IPr})\text{Fe}(\text{NHAr}^{\text{Trip}})(\text{CCC}_6\text{H}_4\text{-}p\text{-CF}_3)]$ (**10**), showing 30% probability ellipsoids and the partial atom-numbering scheme. For simplicity, all hydrogen atoms are omitted. Selected distances (Å) and angles (deg): Fe1–N1 1.922(2), Fe1–C1 2.154(3), Fe1–C2 2.006(3), N1–C37 1.376(3), C2–C29 1.212(4); N1–Fe1–C1 122.92(10), N1–Fe1–C2 135.67(11), C2–Fe1–C1 99.08(10), C37–N1–Fe1 139.24(19).

$\text{C}(\text{sp}^3)\text{-H}$ bonds in these molecules in comparison to the $\text{C}(\text{sp})\text{-H}$ bond in the alkyne. We note that the observed reactivity pattern for **3** is exclusively distinct from those for HAA reactions of Nam's iron(V) imido species, wherein the reaction rate of $\text{C}(\text{sp}^3)\text{-H}$ bond activation decreases as the bond dissociation energy of the target C-H bond increases.⁴² As such, it is *unlikely* that the reaction of **3** with the terminal alkyne involves a direct HAA mechanism. As our calculation study on **3** indicated a high negative charge population on the imido N atom, we reasoned that the polarized N–Fe multiple bond might be amenable to invoke a $[2\pi + 2\sigma]$ -addition pathway to interact with the $\text{H-C}(\text{sp})$ bond and form **10** at the end. Alternatively, a stepwise mechanism that involves the deprotonation of the alkyne by the nucleophilic imido to form iron(II) amido species and alkynyl anion, followed by subsequent binding of the anion to the iron center, could also explain the formation of **9**. Notably, such reactivity is typical of early-transition-metal imido complexes^{83,84} and is rarely known for late-transition-metal imidos.⁴⁷

In contrast to the reluctance of **3** to perform intermolecular $\text{C}(\text{sp}^3)\text{-H}$ bond activation reactions, we found that the interaction of **3** with $(p\text{-Tol})_2\text{CN}_2$ can promote an intramolecular $\text{C}(\text{sp}^3)\text{-H}$ bond activation reaction. Adding 1 equiv of $(p\text{-Tol})_2\text{CN}_2$ in an *n*-hexane solution of **3** at room temperature led to the formation of a brown solution. After workup, the iron(II) amido complex $[(\text{IPr})\text{Fe}(\text{NHAr}^{\text{Trip-H}})]$ (**11**) was isolated as orange crystals in 49% yield (Scheme 6). NMR analysis of the reaction mixture indicated the formation of the azine $(p\text{-Tol})_2\text{CNNC}(p\text{-Tol})_2$ as the byproduct in ca. 45% NMR yield relative to $(p\text{-Tol})_2\text{CN}_2$, which might arise from iron-promoted decomposition of the diazo compound.⁸⁵ The molecular structure of **11** established by XRD clearly shows that the reaction has led to the conversion of the terminal imido ligand $[\text{NAr}^{\text{Trip}}]^{2-}$ of **3** into a bidentate amido-alkyl chelate denoted as $[\text{NHAr}^{\text{Trip-H}}]^{2-}$ in **11** (Figure 8), indicating the involvement of benzylic C-H bond activation on one of the flanking arenes of the imido ligand. The lack of coordination of the diazo ligand $(p\text{-Tol})_2\text{CN}_2$ or its derivatives in **11** suggests that in the course of the intramolecular $\text{C}(\text{sp}^3)\text{-H}$ bond activation reaction the diazo compound seems to play the role of “catalyst” in mediating the C-H activation reaction. Accordingly, it can be proposed that the interaction of **3** with

Scheme 6. $\text{C}(\text{sp}^3)\text{-H}$ Bond Activation Reaction of **3** Triggered by a Diazo Compound and a Proposed Reaction Route

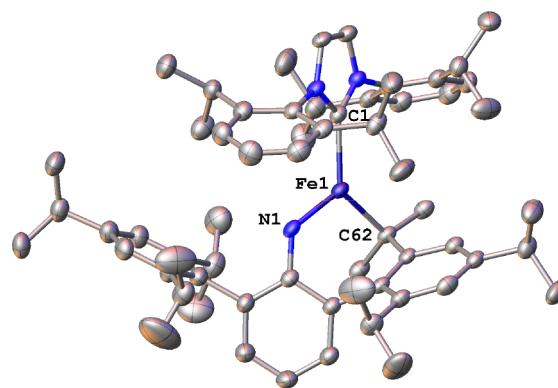
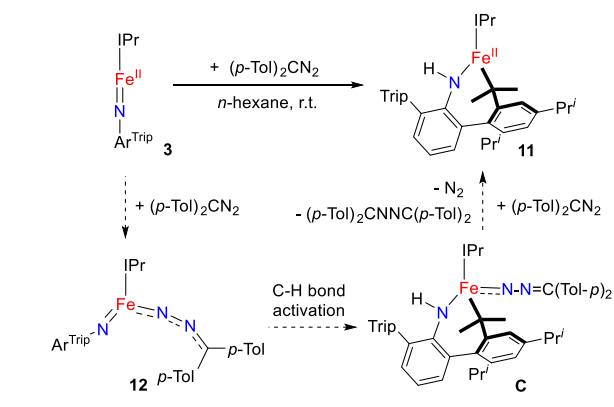


Figure 8. Molecular structure of $[(\text{IPr})\text{Fe}(\text{NHAr}^{\text{Trip-H}})]$ (**11**), showing 30% probability ellipsoids and the partial atom-numbering scheme. For simplicity, only one of the two crystallographically independent molecules in the unit cell is shown and all hydrogen atoms are omitted. Selected distances (Å) and angles (deg): Fe1–N1 1.925(3), Fe1–C1 2.112(3), Fe1–C62 2.092(3); N1–Fe1–C1 120.99(12), N1–Fe1–C62 108.55(12), C62–Fe1–C1 130.42(12), C29–N1–Fe1 124.3(2).

$(p\text{-Tol})_2\text{CN}_2$ might result in the three-coordinate iron imido complex $[(\text{IPr})\text{Fe}(\text{NAr}^{\text{Trip}})(\eta^1\text{-NNC}(\text{To}l\text{-}p)_2)]$ (**12**), which might perform an intramolecular C-H bond activation reaction to form the cyclometalated complex **C**. Complex **C** might be attacked by another molecule of the diazo compound to form cyclometalated complex **11** along with the azine and N_2 (Scheme 6).

Supportive of the aforementioned mechanism, an intermediate, which can further convert into **11**, has been detected from the NMR-scale reaction of **3** with $(p\text{-Tol})_2\text{CN}_2$ (Figure S41). A preparative-scale reaction at -30°C led to the isolation of $[(\text{IPr})\text{Fe}(\text{NAr}^{\text{Trip}})(\eta^1\text{-NNC}(\text{To}l\text{-}p)_2)]$ (**12**). While the low isolated yield and instability of **12** at room temperature do not allow full spectroscopic characterizations, a single-crystal X-ray diffraction study has unambiguously established its structure as a three-coordinate NHC iron imido complex bearing $\eta^1\text{-NNC}(\text{To}l\text{-}p)_2$ ligation. As shown in Figure 9, the coordination of an $\eta^1\text{-NNC}(\text{To}l\text{-}p)_2$ ligand has rendered a face-to-face contact of the flanking arene rings of the NHC ligand with respect to those of the imido ligands in **12**. The Fe–N(imido) distance in **12** (1.707(2) Å) remains close to that in **3** (1.715(2) Å). However, its bent Fe–N(imido)–C(aryl) alignment ($155.79(17)^\circ$) is distinct from the linear

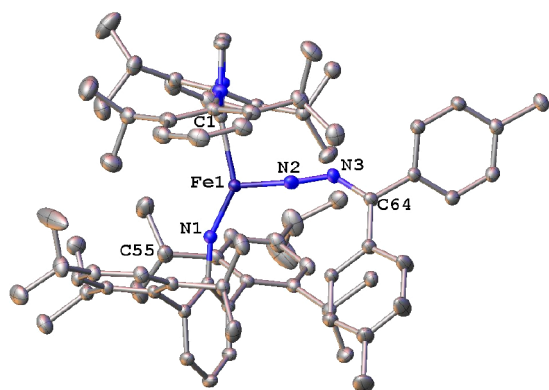


Figure 9. Molecular structure of $[(\text{IPr})\text{Fe}(\text{NAr}^{\text{Trip}})(\eta^1\text{-N}_2\text{C}(\text{Tol-}p)_2)]$ (**12**), showing 30% probability ellipsoids and the partial atom-numbering scheme. For simplicity, all hydrogen atoms are omitted. Selected distances (Å) and angles (deg): Fe1–N1 1.7066(19), Fe1–N2 1.727(2), Fe1–C1 2.061(2), N2–N3 1.248(3), N3–C64 1.308(3); N1–Fe1–C1 141.30(9), N2–Fe1–C1 96.56(9), N1–Fe1–N2 122.07(10), C28–N1–Fe1 155.79(17), N2–N3–C64 135.5(2), N3–N2–Fe1 153.8(2).

Fe–N(imido)–C(aryl) alignment in **3**. Concurrent with the bent Fe–N(imido)–C(aryl) motif, a benzylic C–H bond on the Ar^{Trip} moiety is pointing to the imido N atom, as indicated by their short $\text{N}\cdots\text{C}(55)$ separation of 3.32 Å. The $\eta^1\text{-NNC}(\text{Tol-}p)_2$ ligand in **12** has a short Fe–N(diazo) distance of 1.727(2) Å. Its N–N and N–C distances (1.248(3) and 1.308(3) Å, respectively) and bent N–N–Fe and N–N–C angles (153.8(2) and 135.5(2)°, respectively) are comparable to those of the diazo radical ligands in $[\text{Li}(\text{THF})_4][(\text{tpe})\text{Fe}(\text{NNCPh}_2)]$ (tpe = tris(5-mesitylpyrrolyl)ethane)⁸⁶ and $[\{((\text{Dipp})\text{NC}(\text{Bu}^t))_2\text{CH})\text{Co}(\text{NNCPh}_2)\}]$,⁸⁷ implying the radical anion nature of the $\eta^1\text{-NNC}(\text{Tol-}p)_2$ ligand. Thus, in addition to exertion of a steric effect, the coordination of the diazo ligand might also change the electronic nature of the iron imido moiety. These changes could be beneficial for further intramolecular C(sp³)–H bond activation reactions. It should be noted that at this stage whether the C(sp³)–H bond activation reaction from **12** to **11** undergoes a stepwise mechanism of HAA followed by benzylic radical rebound to iron center or a $[2\pi + 2\sigma]$ -addition mechanism remained unclear. However, the long Fe \cdots C(benzyl) separations in **12** should make it difficult to accommodate a four-membered transition state for the $[2\pi + 2\sigma]$ -addition mechanism.

CONCLUSION

In the present work, we reported the preparation of the first two-coordinate iron(II) imido complex, $[(\text{IPr})\text{Fe}(\text{NAr}^{\text{Trip}})]$, via the reaction of $[(\text{IPr})\text{Fe}(\text{vtms})_2]$ with the bulky organic azide $\text{Ar}^{\text{Trip}}\text{N}_3$. Single-crystal X-ray diffraction revealed a long distance of 1.715(2) Å for its Fe–N multiple bond. Variable-temperature and variable-field magnetometry and ⁵⁷Fe Mössbauer measurements coupled with DFT calculations collectively established an $S = 2$ ground spin state for the two-coordinate iron(II) imido complex, different from Peters' low-spin ($S = 0$) iron(II) imidos with tris(phosphine) ligation.

The iron(II) imido complex $[(\text{IPr})\text{Fe}(\text{NAr}^{\text{Trip}})]$ has been subjected to a detailed reactivity study with the aim of probing the hitherto unknown reactivity of iron(II) imido species. Our study revealed that $[(\text{IPr})\text{Fe}(\text{NAr}^{\text{Trip}})]$ performs nitrene transfer reactions with electron-deficient terminal alkenes and

CO, producing enamines and isocyanide, respectively. In contrast, the interaction of $[(\text{IPr})\text{Fe}(\text{NAr}^{\text{Trip}})]$ with PMe_3 afforded the low-spin iron(II) imido complex $[(\text{Me}_3\text{P})_3\text{Fe}(\text{NAr}^{\text{Trip}})]$ instead of iminophosphine. $[(\text{IPr})\text{Fe}(\text{NAr}^{\text{Trip}})]$ can activate the C(sp)–H bond of a terminal alkyne to afford an alkynyl iron(II) amido complex, whereas it exhibits limited HAA activity toward weaker C–H bonds. When it is treated with a diazo compound, $[(\text{IPr})\text{Fe}(\text{NAr}^{\text{Trip}})]$ can convert into an iron(II) complex bearing a cyclometalated arylamido ligand $[\text{NHAr}^{\text{Trip-H}}]$, wherein an intramolecular HAA reaction might occur.

The outcomes of the aforementioned C–H bond activation reactions and nitrene-transfer reactions with alkenes are different from those of the mid- to high-valent iron imido/iminy complexes. The difference can be attributed to the less covalent iron–imido interaction and the resulting higher negative charge population accumulating on the nitrogen atom of the iron(II) imido complex versus mid- and high-valent iron imidos/iminy complexes as revealed by DFT studies. This bonding feature renders the imido moiety pronounced basicity and nucleophilicity. Equally important is the low-coordinate nature of the metal center, as it might allow the iron center to interact with substrates via a four-membered transition state required for the proposed $[2\pi + 2\sigma]$ -addition mechanism, which is hard to occur with iron imido complexes featuring higher coordination numbers. These results hint at the potential utility of iron(II) imido intermediates for the development of new iron-catalyzed organic transformations.

ASSOCIATED CONTENT

Supporting Information

The Supporting Information is available free of charge on the ACS Publications website at DOI: 10.1021/acs.inorgchem.9b01147.

Detailed experimental procedures, details of the calculation study, characterization data, molecular structures of **1** and **2**, ⁵⁷Fe Mössbauer spectra, NMR spectra, absorption spectra, and electronic configurations of other iron imido species (PDF)

Accession Codes

CCDC 1892821–1892828 contain the supplementary crystallographic data for this paper. These data can be obtained free of charge via www.ccdc.cam.ac.uk/data_request/cif, or by emailing data_request@ccdc.cam.ac.uk, or by contacting The Cambridge Crystallographic Data Centre, 12 Union Road, Cambridge CB2 1EZ, UK; fax: +44 1223 336033.

AUTHOR INFORMATION

Corresponding Authors

*E-mail for S.Y.: shengfa.ye@kofo.mpg.de.

*E-mail for L.D.: deng@sioc.ac.cn.

ORCID

Eckhard Bill: 0000-0001-9138-3964

Shengfa Ye: 0000-0001-9747-1412

Liang Deng: 0000-0002-0964-9426

Notes

The authors declare no competing financial interest.

ACKNOWLEDGMENTS

The work was supported by the National Natural Science Foundation of China (Nos. 21725104, 21690062, 21432001,

and 21821002), the National Key Research and Development Program (2016YFA0202900), and the Strategic Priority Research Program of the Chinese Academy of Sciences (No. XDB20000000). A.S., E.B., and S.Y. gratefully acknowledges the financial support from the Max-Planck Society.

REFERENCES

- (1) Bauer, I.; Knölker, H.-J. Iron Catalysis in Organic Synthesis. *Chem. Rev.* **2015**, *115*, 3170–3387.
- (2) Mehn, M. P.; Peters, J. C. Mid- to High-Valent Imido and Nitrido Complexes of Iron. *J. Inorg. Biochem.* **2006**, *100*, 634–643.
- (3) Che, C.-M.; Zhou, C.-Y.; Wong, E. L.-M. Catalysis by Fe = X Complexes (X = NR, CR₂). *Top. Organomet. Chem.* **2011**, *33*, 111–138.
- (4) Saouma, C. T.; Peters, J. C. M≡E and M=E Complexes of Iron and Cobalt that Emphasize Three-Fold Symmetry (E = O, N, NR). *Coord. Chem. Rev.* **2011**, *255*, 920–937.
- (5) Zhang, L.; Deng, L. C-H Bond Amination by Iron-Imido/Nitrene Species. *Chin. Sci. Bull.* **2012**, *57*, 2352–2360.
- (6) Wang, P.; Deng, L. Recent Advances in Iron-Catalyzed C-H Bond Amination via Iron Imido Intermediate. *Chin. J. Chem.* **2018**, *36*, 1222–1240.
- (7) Nishibayashi, Y. Recent Progress in Transition-Metal-Catalyzed Reduction of Molecular Dinitrogen under Ambient Reaction Conditions. *Inorg. Chem.* **2015**, *54*, 9234–9247.
- (8) Thompson, N. B.; Green, M. T.; Peters, J. C. Nitrogen Fixation via a Terminal Fe(IV) Nitride. *J. Am. Chem. Soc.* **2017**, *139*, 15312–15315.
- (9) McWilliams, S. F.; Bill, E.; Lukat-Rodgers, G.; Rodgers, K. R.; Mercado, B. Q.; Holland, P. L. Effects of N₂ Binding Mode on Iron-Based Functionalization of Dinitrogen to Form an Iron(III) Hydrazido Complex. *J. Am. Chem. Soc.* **2018**, *140*, 8586–8598.
- (10) MacLeod, K. C.; McWilliams, S. F.; Mercado, B. Q.; Holland, P. L. Stepwise N-H Bond Formation from N₂-Derived Iron Nitride, Imide and Amide Intermediates to Ammonia. *Chem. Sci.* **2016**, *7*, 5736–5746.
- (11) Brönstrup, M.; Kretzschmar, I.; Schröder, D.; Schwarz, H. Iron-Mediated Amination of Hydrocarbons in the Gas Phase. *Helv. Chim. Acta* **1998**, *81*, 2348–2369.
- (12) Verma, A. K.; Nazif, T. N.; Achim, C.; Lee, S. C. A Stable Terminal Imide on Iron. *J. Am. Chem. Soc.* **2000**, *122*, 11013–11014.
- (13) Brown, S. D.; Betley, T. A.; Peters, J. C. A Low-Spin d⁵ Iron Imide: Nitrene Capture by Low-Coordinate Iron(I) Provides the 4-Coordinate Fe(III) Complex [PhB(CH₂PPh₂)₃]Fe: N-*p*-tolyl. *J. Am. Chem. Soc.* **2003**, *125*, 322–323.
- (14) Brown, S. D.; Peters, J. C. Hydrogenolysis of [PhBP₃]Fe≡N-*p*-tolyl: Probing the Reactivity of an Iron Imide with H₂. *J. Am. Chem. Soc.* **2004**, *126*, 4538–4539.
- (15) Brown, S. D.; Peters, J. C. Ground-State Singlet L₃Fe-(μ-N)-FeL₃ and L₃Fe(NR) Complexes Featuring Pseudotetrahedral Fe(II) Centers. *J. Am. Chem. Soc.* **2005**, *127*, 1913–1923.
- (16) Lucas, R. L.; Powell, D. R.; Borovik, A. S. Preparation of Iron Amido Complexes via Putative Fe(IV) Imido Intermediates. *J. Am. Chem. Soc.* **2005**, *127*, 11596–11597.
- (17) Bart, S. C.; Lobkovsky, E.; Bill, E.; Chirik, P. J. Synthesis and Hydrogenation of Bis(imino)pyridine Iron Imides. *J. Am. Chem. Soc.* **2006**, *128*, 5302–5303.
- (18) Thomas, C. M.; Mankad, N. P.; Peters, J. C. Characterization of the Terminal Iron(IV) Imides {[PhBP^{tBu}₂(pz′)]Fe^{IV}≡NAd}⁺. *J. Am. Chem. Soc.* **2006**, *128*, 4956–4957.
- (19) Eckert, N. A.; Vaddadi, S.; Stoian, S.; Lachicotte, R. J.; Cundari, T. R.; Holland, P. L. Coordination-Number Dependence of Reactivity in an Imidoiron(III) Complex. *Angew. Chem., Int. Ed.* **2006**, *45*, 6868–6871.
- (20) Ni, C.; Fettinger, J. C.; Long, G. J.; Brynda, M.; Power, P. P. Reaction of a Sterically Encumbered Iron(I) Aryl/Arene with Organoazides: Formation of an Iron(V) Bis(imide). *Chem. Commun.* **2008**, 6045–6047.
- (21) Nieto, I.; Ding, F.; Bontchev, R. P.; Wang, H.; Smith, J. M. Thermodynamics of Hydrogen Atom Transfer to a High-Valent Iron Imido Complex. *J. Am. Chem. Soc.* **2008**, *130*, 2716–2717.
- (22) Cowley, R. E.; Eckert, N. A.; Elhaik, J.; Holland, P. L. Catalytic Nitrene Transfer from an Imidoiron(III) Complex to Form Carbodiimides and Isocyanates. *Chem. Commun.* **2009**, 1760–1762.
- (23) Cowley, R. E.; DeYonker, N. J.; Eckert, N. A.; Cundari, T. R.; DeBeer, S.; Bill, E.; Ottenwaelder, X.; Flaschenriem, C.; Holland, P. L. Three-Coordinate Terminal Imidoiron(III) Complexes: Structure, Spectroscopy, and Mechanism of Formation. *Inorg. Chem.* **2010**, *49*, 6172–6187.
- (24) Cowley, R. E.; Eckert, N. A.; Vaddadi, S.; Figg, T. M.; Cundari, T. R.; Holland, P. L. Selectivity and Mechanism of Hydrogen Atom Transfer by an Isolable Imidoiron(III) Complex. *J. Am. Chem. Soc.* **2011**, *133*, 9796–9811.
- (25) Bowman, A. C.; Milsmann, C.; Bill, E.; Turner, Z. R.; Lobkovsky, E.; DeBeer, S.; Wieghardt, K.; Chirik, P. J. Synthesis and Electronic Structure Determination of *N*-Alkyl-Substituted Bis-(imino)pyridine Iron Imides Exhibiting Spin Crossover Behavior. *J. Am. Chem. Soc.* **2011**, *133*, 17353–17369.
- (26) Moret, M.-E.; Peters, J. C. Terminal Iron Dinitrogen and Iron Imide Complexes Supported by a Tris(phosphino)borane Ligand. *Angew. Chem., Int. Ed.* **2011**, *50*, 2063–2067.
- (27) King, E. R.; Hennessy, E. T.; Betley, T. A. Catalytic C-H Bond Amination from High-Spin Iron Imido Complexes. *J. Am. Chem. Soc.* **2011**, *133*, 4917–4923.
- (28) Cowley, R. E.; Holland, P. L. Ligand Effects on Hydrogen Atom Transfer from Hydrocarbons to Three-Coordinate Iron Imides. *Inorg. Chem.* **2012**, *51*, 8352–8361.
- (29) Leeladee, P.; Jameson, G. N. L.; Siegler, M. A.; Kumar, D.; de Visser, S. P.; Goldberg, D. P. Generation of a High-Valent Iron Imido Corrolazine Complex and NR Group Transfer Reactivity. *Inorg. Chem.* **2013**, *52*, 4668–4682.
- (30) Searles, K.; Fortier, S.; Khusniyarov, M. M.; Carroll, P. J.; Sutter, J.; Meyer, K.; Mendiola, D. J.; Caulton, K. G. A *cis*-Divacant Octahedral and Mononuclear Iron(IV) Imide. *Angew. Chem., Int. Ed.* **2014**, *53*, 14139–14143.
- (31) Zhang, H.; Ouyang, Z.; Liu, Y.; Zhang, Q.; Wang, L.; Deng, L. Aminocarbene(Divinyltetramethyldisiloxane)Iron(0) Compounds: A Class of Low-coordinate Iron(0) Reagents. *Angew. Chem., Int. Ed.* **2014**, *53*, 8432–8436.
- (32) Kuppuswamy, S.; Powers, T. M.; Johnson, B. M.; Brozek, C. K.; Krogman, J. P.; Bezpalko, M. W.; Berben, L. A.; Keith, J. M.; Foxman, B. M.; Thomas, C. M. One-Electron Oxidation Chemistry and Subsequent Reactivity of Diiron Imido Complexes. *Inorg. Chem.* **2014**, *53*, 5429–5437.
- (33) Wang, L.; Hu, L.; Zhang, H.; Chen, H.; Deng, L. Three-Coordinate Iron(IV) Bisimido Complexes with Aminocarbene Ligand: Synthesis, Structure, and Reactivity. *J. Am. Chem. Soc.* **2015**, *137*, 14196–14207.
- (34) Iovan, D. A.; Betley, T. A. Characterization of Iron-Imido Species Relevant for *N*-Group Transfer Chemistry. *J. Am. Chem. Soc.* **2016**, *138*, 1983–1993.
- (35) Wilding, M. J. T.; Iovan, D. A.; Wrobel, A. T.; Lukens, J. T.; MacMillan, S. N.; Lancaster, K. M.; Betley, T. A. Direct Comparison of C-H Bond Amination Efficacy through Manipulation of Nitrogen-Valence Centered Redox: Imido versus Iminyl. *J. Am. Chem. Soc.* **2017**, *139*, 14757–14766.
- (36) Jacobs, B. P.; Wolczanski, P. T.; Jiang, Q.; Cundari, T. R.; MacMillan, S. N. Rare Examples of Fe(IV) Alkyl-Imide Migratory Insertions: Impact of Fe-C Covalency in (Me₂IPr)Fe(=NAD)R₂ (R = ^{nec}Pe, 1-nor). *J. Am. Chem. Soc.* **2017**, *139*, 12145–12148.
- (37) Wilding, M. J. T.; Iovan, D. A.; Betley, T. A. High-Spin Iron Imido Complexes Competent for C-H Bond Amination. *J. Am. Chem. Soc.* **2017**, *139*, 12043–12049.
- (38) Kuppuswamy, S.; Powers, T. M.; Johnson, B. M.; Bezpalko, M. W.; Brozek, C. K.; Foxman, B. M.; Berben, L. A.; Thomas, C. M. Metal-Metal Interactions in C₃-Symmetric Diiron Imido Complexes

Linked by Phosphinoamide Ligands. *Inorg. Chem.* **2013**, *52*, 4802–4811.

(39) Bucinsky, L.; Breza, M.; Lee, W.-T.; Hickey, A. K.; Dickie, D. A.; Nieto, I.; DeGayner, J. A.; Harris, T. D.; Meyer, K.; Krzystek, J.; Ozarowski, A.; Nehrkorn, J.; Schnegg, A.; Holldack, K.; Herber, R. H.; Telsler, J.; Smith, J. M. Spectroscopic and Computational Studies of Spin States of Iron(IV) Nitrido and Imido Complexes. *Inorg. Chem.* **2017**, *56*, 4751–4768.

(40) Klinker, E. J.; Jackson, T. A.; Jensen, M. P.; Stubna, A.; Juhász, G.; Bominaar, E. L.; Münck, E.; Que, L., Jr. A Tosylimido Analogue of a Nonheme Oxoiron(IV) Complex. *Angew. Chem., Int. Ed.* **2006**, *45*, 7394–7397.

(41) Hong, S.; Lu, X.; Lee, Y.-M.; Seo, M. S.; Ohta, T.; Ogura, T.; Clémancey, M.; Maldivi, P.; Latour, J.-M.; Sarangi, R.; Nam, W. Achieving One-Electron Oxidation of a Mononuclear Nonheme Iron(V)-Imido Complex. *J. Am. Chem. Soc.* **2017**, *139*, 14372–14375.

(42) Hong, S.; Sutherland, K. D.; Vardhaman, A. K.; Yan, J. J.; Park, S.; Lee, Y.-M.; Jang, S.; Lu, X.; Ohta, T.; Ogura, T.; Solomon, E. I.; Nam, W. A Mononuclear Nonheme Iron(V)-Imido Complex. *J. Am. Chem. Soc.* **2017**, *139*, 8800–8803.

(43) Hennessy, E. T.; Liu, R. Y.; Iovan, D. A.; Duncan, R. A.; Betley, T. A. Iron-Mediated Intermolecular N-Group Transfer Chemistry with Olefinic Substrates. *Chem. Sci.* **2014**, *5*, 1526–1532.

(44) King, E. R.; Hennessy, E. T.; Betley, T. A. Catalytic C-H Bond Amination from High-Spin Iron Imido Complexes. *J. Am. Chem. Soc.* **2011**, *133*, 4917–4923.

(45) Wigley, D. E.; Karlin, K. D. Organoimido Complexes of the Transition Metals. *Prog. Inorg. Chem.* **2007**, *42*, 239–482.

(46) Mindiola, D. J. Oxidatively Induced Abstraction Reactions. A Synthetic Approach to Low-Coordinate and Reactive Early Transition Metal Complexes Containing Metal-Ligand Multiple Bonds. *Acc. Chem. Res.* **2006**, *39*, 813–821.

(47) Du, J.; Wang, L.; Xie, M.; Deng, L. A Two-Coordinate Cobalt(II) Imido Complex with NHC Ligation: Synthesis, Structure, and Reactivity. *Angew. Chem., Int. Ed.* **2015**, *54*, 12640–12644.

(48) Yao, X.; Du, J.; Zhang, Y.; Leng, X.; Yang, M.; Jiang, S.; Wang, Z.; Ouyang, Z.; Deng, L.; Wang, B.; Gao, S. Two-Coordinate Co(II) Imido Complexes as Outstanding Single-Molecule Magnets. *J. Am. Chem. Soc.* **2017**, *139*, 373–380.

(49) Twamley, B.; Hwang, C.-S.; Hardman, N. J.; Power, P. P. Sterically Encumbered Terphenyl Substituted Primary Pnictanes ArEH₂ and Their Metallated Derivatives ArE(H)Li (Ar = C₆H₃-2,6-Trip₂; Trip = 2,4,6-triisopropylphenyl; E = N, P, As, Sb). *J. Organomet. Chem.* **2000**, *609*, 152–160.

(50) Holland, P. L. Electronic Structure and Reactivity of Three-Coordinate Iron Complexes. *Acc. Chem. Res.* **2008**, *41*, 905–914.

(51) Mo, Z.; Deng, L. Open-Shell Iron Hydrocarbyls. *Coord. Chem. Rev.* **2017**, *350*, 285–299.

(52) Laskowski, C. A.; Miller, A. J. M.; Hillhouse, G. L.; Cundari, T. R. A Two-Coordinate Nickel Imido Complex That Effects C-H Amination. *J. Am. Chem. Soc.* **2011**, *133*, 771–773.

(53) Ingleson, M. J.; Layfield, R. A. N-Heterocyclic Carbene Chemistry of Iron: Fundamentals and Applications. *Chem. Commun.* **2012**, *48*, 3579–3589.

(54) Riener, K.; Haslinger, S.; Raba, A.; Högerl, M. P.; Cokoja, M.; Herrmann, W. A.; Kühn, F. E. Chemistry of Iron N-Heterocyclic Carbene Complexes: Syntheses, Structures, Reactivities, and Catalytic Applications. *Chem. Rev.* **2014**, *114*, 5215–5272.

(55) Ouyang, Z.; Du, J.; Wang, L.; Kneebone, J. L.; Neidig, M. L.; Deng, L. Linear and T-Shaped Iron(I) Complexes Supported by N-Heterocyclic Carbene Ligands: Synthesis and Structure Characterization. *Inorg. Chem.* **2015**, *54*, 8808–8816.

(56) Lipschutz, M. I.; Chantarojsiri, T.; Dong, Y.; Tilley, T. D. Synthesis, Characterization, and Alkyne Trimerization Catalysis of a Heteroleptic Two-Coordinate Fe^I Complex. *J. Am. Chem. Soc.* **2015**, *137*, 6366–6372.

(57) Zadrozny, J. M.; Atanasov, M.; Bryan, A. M.; Lin, C.-Y.; Rekker, B. D.; Power, P. P.; Neese, F.; Long, J. R. Slow Magnetization

Dynamics in a Series of Two-Coordinate Iron(II) Complexes. *Chem. Sci.* **2013**, *4*, 125–138.

(58) Chilton, N. F.; Lei, H.; Bryan, A. M.; Grandjean, F.; Long, G. J.; Power, P. P. Ligand Field Influence on the Electronic and Magnetic Properties of Quasi-Linear Two-Coordinate Iron(II) Complexes. *Dalton Trans.* **2015**, *44*, 11202–11211.

(59) Lin, C.-Y.; Guo, J.-D.; Fettinger, J. C.; Nagase, S.; Grandjean, F.; Long, G. J.; Chilton, N. F.; Power, P. P. Dispersion Force Stabilized Two-Coordinate Transition Metal-Amido Complexes of the -N(SiMe₃)Dipp (Dipp = C₆H₃-2,6-Prⁱ₂) Ligand: Structural, Spectroscopic, Magnetic, and Computational Studies. *Inorg. Chem.* **2013**, *52*, 13584–13593.

(60) Zadrozny, J. M.; Xiao, D. J.; Long, J. R.; Atanasov, M.; Neese, F.; Grandjean, F.; Long, G. J. Mössbauer Spectroscopy as a Probe of Magnetization Dynamics in the Linear Iron(I) and Iron(II) Complexes [Fe(C(SiMe₃)₃)₂]^{1-/0}. *Inorg. Chem.* **2013**, *52*, 13123–13131.

(61) Bryan, A. M.; Lin, C.-Y.; Sorai, M.; Miyazaki, Y.; Hoyt, H. M.; Hablutzel, A.; LaPointe, A.; Reiff, W. M.; Power, P. P.; Schulz, C. E. Measurement of Extreme Hyperfine Fields in Two-Coordinate High-Spin Fe²⁺ Complexes by Mössbauer Spectroscopy: Essentially Free-Ion Magnetism in the Solid State. *Inorg. Chem.* **2014**, *53*, 12100–12107.

(62) Reiff, W. M.; Schulz, C. E.; Whangbo, M.-H.; Seo, J. I.; Lee, Y. S.; Potratz, G. R.; Spicer, C. W.; Girolami, G. S. Consequences of a Linear Two-Coordinate Geometry for the Orbital Magnetism and Jahn-Teller Distortion Behavior of the High Spin Iron(II) Complex Fe[N(t-Bu)₂]₂. *J. Am. Chem. Soc.* **2009**, *131*, 404–405.

(63) Reiff, W. M.; LaPointe, A. M.; Witten, E. H. Virtual Free Ion Magnetism and the Absence of Jahn-Teller Distortion in a Linear Two-Coordinate Complex of High-Spin Iron(II). *J. Am. Chem. Soc.* **2004**, *126*, 10206–10207.

(64) Merrill, W. A.; Stich, T. A.; Brynda, M.; Yeagle, G. J.; Fettinger, J. C.; De Hont, R.; Reiff, W. M.; Schulz, C. E.; Britt, R. D.; Power, P. P. Direct Spectroscopic Observation of Large Quenching of First-Order Orbital Angular Momentum with Bending in Monomeric, Two-Coordinate Fe(II) Primary Amido Complexes and the Profound Magnetic Effects of the Absence of Jahn- and Renner-Teller Distortions in Rigorously Linear Coordination. *J. Am. Chem. Soc.* **2009**, *131*, 12693–12702.

(65) Chow, T. W.-S.; Chen, G.-Q.; Liu, Y.; Zhou, C.-Y.; Che, C.-M. Practical Iron-Catalyzed Atom/Group Transfer and Insertion Reactions. *Pure Appl. Chem.* **2012**, *84*, 1685–1704.

(66) Gober, J. G.; Brustad, E. M. Non-Natural Carbenoid and Nitrenoid Insertion Reactions Catalyzed by Heme Proteins. *Curr. Opin. Chem. Biol.* **2016**, *35*, 124–132.

(67) Cramer, S. A.; Jenkins, D. M. Synthesis of Aziridines from Alkenes and Aryl Azides with a Reusable Macrocyclic Tetracarbene Iron Catalyst. *J. Am. Chem. Soc.* **2011**, *133*, 19342–19345.

(68) Fingerhut, A.; Serdyuk, O. V.; Tsogoeva, S. B. Non-Heme Iron Catalysts for Epoxidation and Aziridination Reactions of Challenging Terminal Alkenes: Towards Sustainability. *Green Chem.* **2015**, *17*, 2042–2058.

(69) Day, B. M.; Pugh, T.; Hendriks, D.; Guerra, C. F.; Evans, D. J.; Bickelhaupt, F. M.; Layfield, R. A. Normal-to-Abnormal Rearrangement and NHC Activation in Three-Coordinate Iron(II) Carbene Complexes. *J. Am. Chem. Soc.* **2013**, *135*, 13338–13341.

(70) Park, S. H.; Kwak, J.; Shin, K.; Ryu, J.; Park, Y.; Chang, S. Mechanistic Studies of the Rhodium-Catalyzed Direct C-H Amination Reaction Using Azides as the Nitrogen Source. *J. Am. Chem. Soc.* **2014**, *136*, 2492–2502.

(71) Park, Y.; Kim, Y.; Chang, S. Transition Metal-Catalyzed C-H Amination: Scope, Mechanism, and Applications. *Chem. Rev.* **2017**, *117*, 9247–9301.

(72) Waterman, R.; Hillhouse, G. L. Group Transfer from Nickel Imido, Phosphinidene, and Carbene Complexes to Ethylene with Formation of Aziridine, Phosphirane, and Cyclopropane Products. *J. Am. Chem. Soc.* **2003**, *125*, 13350–13351.

(73) Wang, X.; Mo, Z.; Xiao, J.; Deng, L. Monomeric Bis(anilido)-iron(II) Complexes with *N*-Heterocyclic Carbene Ligation: Synthesis, Characterization, and Redox Reactivity toward Aryl Halides. *Inorg. Chem.* **2013**, *52*, 59–65.

(74) Singh, A. K.; Levine, B. G.; Staples, R. J.; Odom, A. L. A 4-Coordinate Ru(II) Imido: Unusual Geometry, Synthesis, and Reactivity. *Chem. Commun.* **2013**, *49*, 10799–10801.

(75) Liu, Y.; Du, J.; Deng, L. Synthesis, Structure, and Reactivity of Low-Spin Cobalt(II) Imido Complexes [(Me₃P)₃Co(NAr)]. *Inorg. Chem.* **2017**, *56*, 8278–8286.

(76) Scepianiak, J. J.; Margarit, C. G.; Harvey, J. N.; Smith, J. M. Nitrogen Atom Transfer from Iron(IV) Nitrido Complexes: A Dual-Nature Transition State for Atom Transfer. *Inorg. Chem.* **2011**, *50*, 9508–9517.

(77) Lai, W.; Li, C.; Chen, H.; Shaik, S. Hydrogen-Abstraction Reactivity Patterns from A to Y: The Valence Bond Way. *Angew. Chem., Int. Ed.* **2012**, *51*, 5556–5578.

(78) Mayer, J. M. Understanding Hydrogen Atom Transfer: From Bond Strengths to Marcus Theory. *Acc. Chem. Res.* **2011**, *44*, 36–46.

(79) Vardhaman, A. K.; Barman, P.; Kumar, S.; Sastri, C. V.; Kumar, D.; de Visser, S. P. Comparison of the Reactivity of Nonheme Iron(IV)-Oxo versus Iron(IV)-Imido Complexes: Which is the Better Oxidant? *Angew. Chem., Int. Ed.* **2013**, *52*, 12288–12292.

(80) Kumar, S.; Faponle, A. S.; Barman, P.; Vardhaman, A. K.; Sastri, C. V.; Kumar, D.; de Visser, S. P. Long-Range Electron Transfer Triggers Mechanistic Differences between Iron(IV)-Oxo and Iron(IV)-Imido Oxidants. *J. Am. Chem. Soc.* **2014**, *136*, 17102–17115.

(81) Vardhaman, A. K.; Lee, Y.-M.; Jung, J.; Ohkubo, K.; Nam, W.; Fukuzumi, S. Enhanced Electron Transfer Reactivity of a Nonheme Iron(IV)-Imido Complex as Compared to the Iron(IV)-Oxo Analogue. *Angew. Chem., Int. Ed.* **2016**, *55*, 3709–3713.

(82) Spasyuk, D. M.; Carpenter, S. H.; Kefalidis, C. E.; Piers, W. E.; Neidig, M. L.; Maron, L. Facile Hydrogen Atom Transfer to Iron(III) Imido Radical Complexes Supported by a Dianionic Pentadentate Ligand. *Chem. Sci.* **2016**, *7*, 5939–5944.

(83) Ochi, N.; Nakao, Y.; Sato, H.; Sakaki, S. Theoretical Study of C-H and N-H σ -bond Activation Reactions by Titanium(IV)-Imido Complex. Good Understanding Based on Orbital Interaction and Theoretical Proposal for N-H σ -Bond Activation of Ammonia. *J. Am. Chem. Soc.* **2007**, *129*, 8615–8624.

(84) Ochi, N.; Nakao, Y.; Sato, H.; Sakaki, S. Theoretical Prediction of O-H, Si-H, and Si-C σ -Bond Activation Reactions by Titanium(IV)-Imido Complex. *Can. J. Chem.* **2009**, *87*, 1415–1424.

(85) Safari, J.; Gandomi-Ravandi, S. Structure, Synthesis and Application of Azines: A Historical Perspective. *RSC Adv.* **2014**, *4*, 46224–46249.

(86) Sazama, G. T.; Betley, T. A. Multiple, Disparate Redox Pathways Exhibited by a Tris(pyrrolido)ethane Iron Complex. *Inorg. Chem.* **2014**, *53*, 269–281.

(87) Bonyhady, S. J.; Goldberg, J. M.; Wedgwood, N.; Dugan, T. R.; Eklund, A. G.; Brennessel, W. W.; Holland, P. L. Cobalt(II) Complex of a Diazoalkane Radical Anion. *Inorg. Chem.* **2015**, *54*, 5148–5150.